Rev.Adv.Mater.Sci. 8 (2004) 152-157

STRUCTURE AND ELECTRICAL PROPERTIES OF CoFeZr-ALUMINIUM OXIDE NANOCOMPOSITE FILMS

A.M. Saad [1], A.V. Mazanik [2], Yu.E. Kalinin [3], J.A. Fedotova [4], A.K. Fedotov [2], S. Wrotek [5], A.V. Sitnikov [3] and I.A. Svito [2]

[1]Al-Balqa Applied University, P.O.Box 2041, Amman 11953, Jordan
[2]Belarusian State University, F. Skaryna av. 4, 220050 Minsk, Belarus
[3]Voronezh State Technical University, 250770 Voronez, Russia
[4]National Centre for High Energy and Particle Physics of Belarusian State University, 153 M. Bogdanovich str., 220040 Minsk, Belarus
[5]Institute of Physics, Polish Academy of Sciences, 02-668 Warsaw, Poland

Recieved: December 14, 2004

Abstract. The influence of composition on DC carrier transport of composite films containing amorphous CoFeZr nanoparticles in amorphous aluminium oxide matrix has been investigated. The films in the range of 3 to 5 μm thick with variable composition were sputtered on single substrate from the compound target in the chamber with argon-oxygen gas mixture. TEM, SEM and Mössbauer spectroscopy have shown that all the studied films of $(Co_{0.45}Fe_{0.45}Zr_{0.10})_X(Al_2O_3)_{1-X}$ with 30 at.% < X < 65 at.% revealed structure with distributed fragmented components of amorphous metallic alloy (with dimensions of particles between 6 and 10 nm) and amorphous alumina. The presence of two critical regions for metallic fraction (X_1 = 33 - 40 at.% and X_2 = 50 - 55 at.%), where diagram 'electric property-composition' exhibit pronounced peculiarities, has been revealed. A qualitative structural model of nanocomposite is offered to explain this behavior. In accordance with the model the first critical region is connected with the delay of percolation threshold due to partial oxidation of metallic nanoparticles during sputtering. The second critical region of composition is ascribed to the formation of percolative net of amorphous metallic nanoparticles in dielectric alumina matrix.

1. INTRODUCTION

At present time high interest is given to nanostructured materials, which consist of metallic nanosized granules randomly distributed within a dielectric matrix, because of their unusual magnetic, electrical, optical and magneto-optical properties. There are very important features of nanocomposites such as the ability to change their resistance in a wide range, high absorbance of electro-magnetic irradiation at high and extremely high frequencies, characteristic properties of magnetotransport of carriers (gigantic and negative magnetoresistance), etc. The latter, in particular, allows one to ascribe such composites to spintronic materials that are very perspective as materials for manufacturing of magnetic heads for recording and reproduction of information. Moreover, a practical interest to nanocomposites is conditioned on their implementation as protective coatings and for other goals as well. Considerable recent attention has been focused on amorphous alloys on the base of iron and cobalt which display m-metal properties at low frequencies. However, their application at high frequencies is impeded to increase the eddy currents losses. In order to decrease these losses one needs to increase resistivity of magnetic alloys and that is possible by means of preparation of metal-dielectric nanocomposites with insulating matrixes (stuffs) like SiO_2 or Al_2O_3.

Corresponding author: A.K. Fedotov, e-mail: fedotov@bsu.by

Goal of the present paper is to investigate the influence of composition on DC carrier transport of the composites films containing amorphous CoFeZr nanoparticles in amorphous aluminium oxide matrix.

2. EXPERIMENTAL

The studied samples of $(Co_{0.45}Fe_{0.45}Zr_{0.10})_X(Al_2O_3)_{1-X}$ with 30 at.% < *X* < 65 at.% were manufactured as films in the range of 3 to 5 μm thick using ion-beam sputtering of the compound target onto the motionless water cooled substrate with argon and oxygen gas mixture in the chamber. The pressure of the gas mixture in the chamber was $9.6 \cdot 10^{-2}$ Pa at the oxygen partial pressure of $4.41 \cdot 10^{-2}$ Pa. The original configuration of the compound target enabled us to prepare composite film with different metallic to dielectric components ratio in one technological process [1].

Measurements of content of the chemical elements belonging to the composites were carried out using a special micro-probe X-Ray analysis. The structure of the as-deposited composites was investigated using transmission (TEM) and scanning (SEM) electron microscopes. Structural characterization (phase composition and also the valence state of Fe ions) were also performed with the help of Mössbauer spectroscopy. Mössbauer spectra were recorded in transmission geometry at room temperature using spectrometer MS2000 with ^{57}Fe/Rh source and $YAlO_3$:Ce crystalline scintillation detector. Spectra were treated with the MOSMOD code [2] that allowed taking into account distribution of quadrupole splitting (QS). The width of Lorenz lines, describing individual crystallographically inequivalent positions of iron ions, assumed to be identical for all subspectra and equal to 0.14 mm/s. All isomeric shifts (IS) indicated relatively to α-Fe and set of spectra statistics were (3 to 5)·10^6 pulses.

The studied samples (films) were sputtered onto glassceramic substrates (for electric measurements) and thin aluminium foils (for Mössbauer investigation). The nanocomposite films deposited onto glassceramic substrates were cut into rectangular strips of 10 mm long and 2 mm wide in order to make measurements of DC conductance in the longitudinal geometry at the temperature of 77-300K for electric field intensities *E* up to 10^5 V/m and magnetic fields with induction *B* up to 600 mT.

TEM microscopy of as-deposited films revealed their fragmented structure with distributed components of amorphous metallic alloy (with dimensions of particles between 6 and 10 nm) and amorphous alumina [1].

3. RESULTS AND DISCUSSION

Mössbauer spectra of the studied samples with atomic fraction of $Co_{0.45}Fe_{0.45}Zr_{0.10}$ nanoparticles ranged between 39 at.% and 64 at.% are presented in Fig. 1. Interpretation of the spectra with metallic

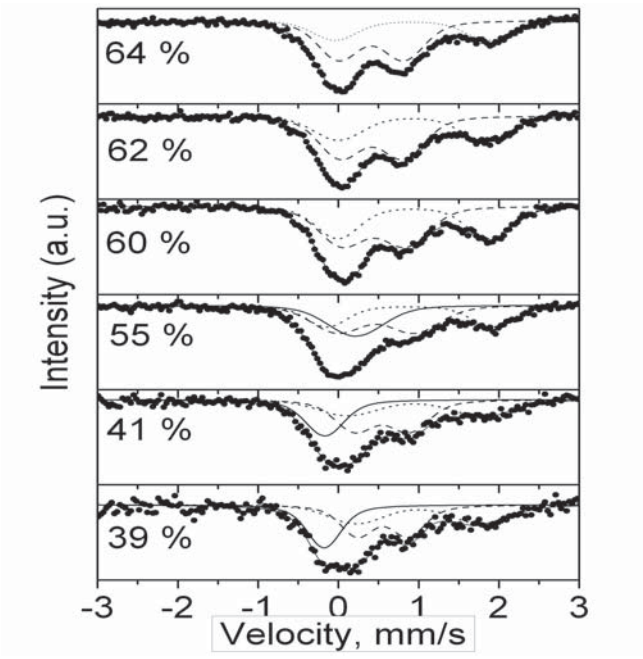

Fig. 1. Mössbauer spectra (points) and their fittings (solid, dashed and dotted subspectra) for nanocomposites with *X* = 39 - 64 at.%.

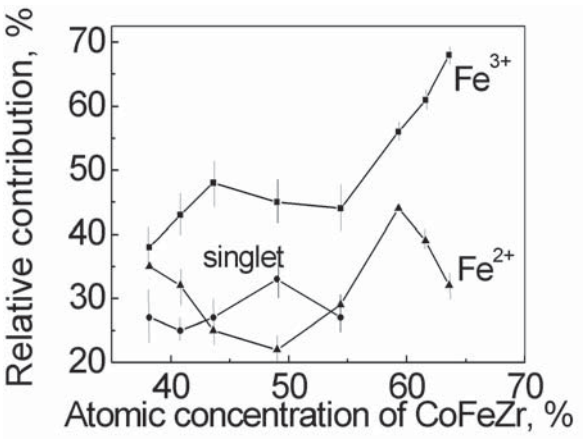

Fig. 2. Relative contributions of local iron configurations *vs* metallic nanoparticles percentage for the samples of $(Co_{0.45}Fe_{0.45}Zr_{0.10})_X(Al_2O_3)_{1-X}$ with X = 39 - 64 at.%.

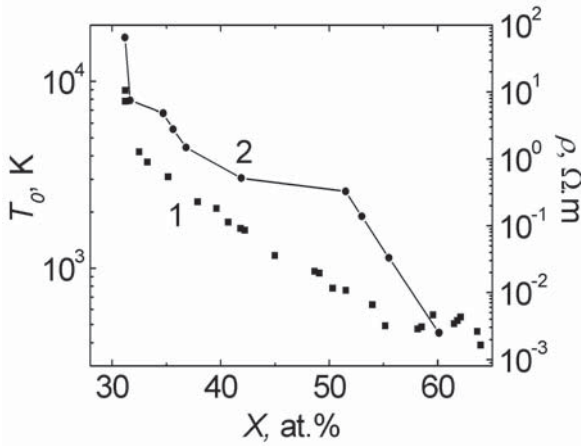

Fig. 3. Resistivity at 295K (1) and characteristic temperature T_o in Mott law for T < 180K (2) *vs* atomic concentration of metallic component.

fraction less than 39 at.% was difficult due to low concentration of ^{57}Fe ions and correspondent spectra are not shown here.

For composites with X > 55 at.% satisfactory computer fitting of the spectra for all the studied samples has been made in assumption of the presence of two quadrupole doublets characterizing different valence states of iron ions - Fe^{2+} (dotted subspectra in Fig. 1) and Fe^{3+} (dashed subspectra in Fig. 1). For the composites with $X \leq 55$ at.% the presence of additional single line component (solid subspectra in Fig. 1) has been observed. Fig. 2 shows variations of relative fractions of two doublets and singlet extracted from Mössbauer spectra with atomic fraction of $Co_{0.45}Fe_{0.45}Zr_{0.10}$.

An attempt to identify the revealed local configurations of Fe ions was carried out by analyzing of respective hyperfine parameters and contributions for different X (Fig. 2). In particular, single line observed on spectra of the samples with X < 55 at.% most probably should be attributed to nanoclusters of $Co_{0.45}Fe_{0.45}Zr_{0.10}$ demonstrating superparamagnetic relaxation at room temperature. The Fe^{3+} doublet was characterized by the values of IS in the range of 0.41-0.56 mm/s and QS between 0.63 and 0.95 mm/s. The wide range of hyperfine parameter values made the interpretation of Fe^{3+}-containing phases quite ambiguous.

Extracted from subspectra values of IS and QS allow to propose at least three possible interpretations of the Fe^{3+} doublet appearance. Firstly, one can assume formation of Fe-containing oxide nanoprecipitates around metallic nanoparticles due to high partial pressure of oxygen in a chamber during film deposition [1,3]. Secondly, this doublet can characterize Fe^{3+} ions incorporated into alumina matrix [4]. Finally, variation of relative fraction of Fe^{3+} doublet (see Fig. 2) is evidenced of its strong correlation with atomic fraction of $Co_{0.45}Fe_{0.45}Zr_{0.10}$ nanoparticles. This fact allowed us to suppose that considered doublet characterizes $Co_{0.45}Fe_{0.45}Zr_{0.10}$ phase whose structure differs from those characterized by single line.

The doublet which characterizes Fe^{2+} valence configuration shows that the IS and QS values varied in the range of 0.88-1.10 and 1.55-2.09 mm/s, respectively. The data presented in [5] showed that the interaction of iron nanoparticles with Al_2O_3 matrix may cause the formation of $FeAl_2O_4$ compound (hercinite).

Summarizing the Mössbauer spectroscopy data, the main features can be noted as follows: coexistence of Fe ions in two valence states – Fe^{2+} and Fe^{3+}; the pronounced tendency to the increase of Fe^{3+} fraction with the X growth; disappearing of singlet connected with Fe-containing nanoparticles for the samples with X > 55 at.%. The important feature of Mössbauer spectra was the lack of ferromagnetic state in the metallic nanoparticles.

The behavior of conductance at room temperature *vs.* metallic phase concentration is presented in Fig. 3 (curve 1). The low temperature study has shown (see Fig. 4) that, for all the investigated concentrations X of metallic fraction in nanocomposites, the temperature dependences of the conductance in the range of 80-300K display a behavior agreed

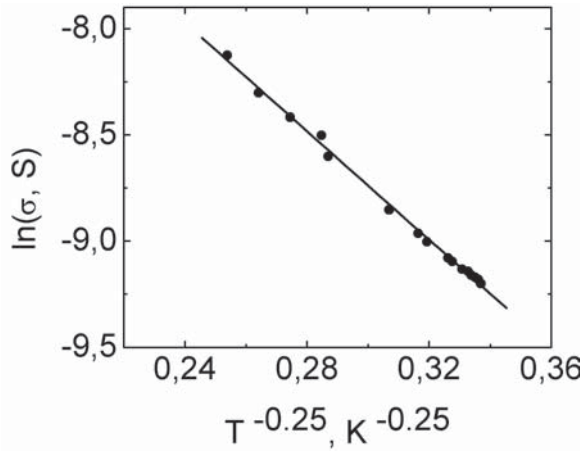

Fig. 4. Temperature dependence of conductance for nanocomposite with X = 35 at.%.

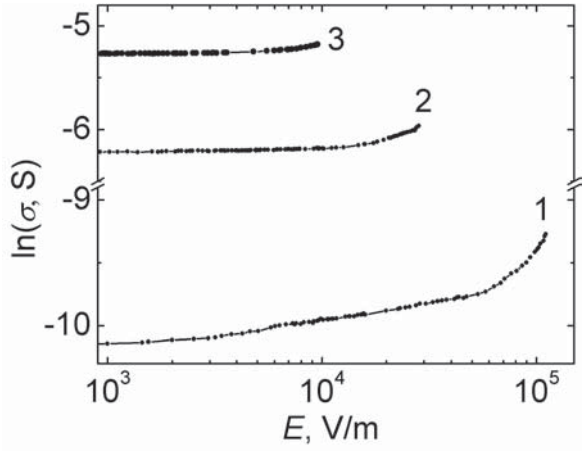

Fig. 5. Conductance at 295K *vs* electric field intensity for nanocomposites with X = 35 (1), 51 (2) and 62 at.% (3).

closely to the formula $\ln(\sigma) \propto (T_o/T)^n$ [6] for n = 0.25 at T<180K and for n = 0.5 at T>180K. The mentioned results testify that the carrier transport in the composites is predominantly carried out by thermally-activated tunneling (hopping) over localised states following either Mott law (for n = 0.25) [6] or Shklovski-Efros law (n = 0.5) [7]. In this case the characteristic temperature T_o can serve as characteristics of the activation energy of conductance in the working temperature range where hopping mechanism of carriers is taking place (see curve 2 in Fig. 3).

For the studied temperature range, the electric field dependencies of DC conductance σ show a non-Ohmic behavior with features of thermal avalanche at electric fields $E > 10^4$ V/m (Fig. 5). In the region of $E < 10^4$ V/m these σ(E) dependencies, to a high accuracy, could be fitted by a sum of exponential Hill law $\ln(\sigma) \propto erE/kT$ (e – electron charge, r – range of electron hopping, k – Boltzman constant) [8] and usual Ohmic contribution. This allowed the exponential contribution to increase as the metallic component concentration decreased in the nanocomposite. The hopping range r in different composites was calculated by using the above-mentioned fitting method as presented in Fig. 6 (curve 1). Note that for composites with X > 40 at.% Ohmic behavior (linear contribution to current-voltage characteristics) become stronger with the lowering of temperature.

Magnetoresistance (MR) for the whole region of the studied nancomposites at room temperature was negative obeying the relationship of $[\Delta R(B)/R(0)] \propto -B^k$ with magnetic induction B growth, as shown in Fig. 7. Negative sign of MR and the exponent k, which is close to 2 (as shown in Fig. 6 - curve 2), are evidence of the tunnel character of the carrier transport in the studied nanocomposites [9].

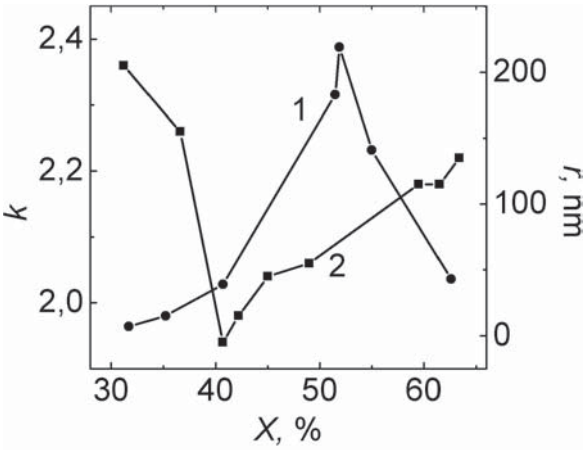

Fig. 6. Hopping range of carriers r (1) and exponent k in magnetic field dependence of resistance (2) *vs* metallic fraction X.

The study of electrical properties and Mössbauer spectra show the presence of two critical regions (X_1 = 33 - 40 at.% and X_2 = 50 - 55 at.%) for the metallic phase concentration X where 'property-composition' dependencies exhibit peculiarities such as sharp bend or sudden change (extreme). The above figures for the X_1 critical region curves $r(X)$ and $T_o(X)$ display sharp bend (Fig. 3) but $k(X)$ shows minimum (curve 2 in Fig. 6). At the same time, for the

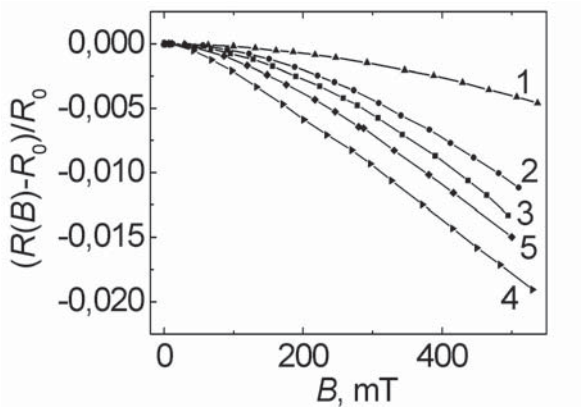

Fig. 7. Reduced resistance *vs* magnetic induction *B* for nanocomposites with X = 33.3 (1), 48.7 (2), 57.1 (3), 55.2 (4) and 58.2 at.% (5).

X_2 critical region curves r(X) and $T_o(X)$ display the second sharp bend (Fig. 3) and dependences $r(X)$ show maximum (curve 1 in Fig. 6). Moreover, just in this region of metallic phase concentration the singlet on Mössbauer spectra disappeared (Fig. 2).

In this context, the concentration region X_1 can be viewed as a boundary between the composite state with a random distribution of metallic nanoparticles (Fig. 8a) and the state where percolation cluster could be evolved from metallic nanoparticles assuming that these particles could be partially oxidized (due to the presence of oxygen in a gas mixture in a chamber). In other words, as shown in Fig. 8b, most of the nanoparticles are in a close contact with each other but some of them are disconnected electrically by oxide precipitates. This avoided the formation of a continuous percolation cluster in the composite that resulted in the rise of barrier for DC carrier transport and shifted the real percolation threshold to higher concentrations of metallic phase. Thus the region X_1 can be treated as any pre-percolation state of the studied nanocomposite when they are still on the dielectric side of metal-nonmetal transition. Further increase of the metallic fraction near the X_2 region (Fig. 8c) allowed the composites to pass fully into the metallic state (to be beyond the percolation threshold) and that resulted in sharp decrease of the parameter T_o (curve 2 in Fig. 3) and hopping range r of carriers (curve 1 in Fig. 6) for low temperature DC carrier transport. Finally, at $X > X_2$ the whole percolative net was probably formed from pre-percolation clusters disconnected earlier by oxide precipitates (Fig. 8d). The latter was just confirmed by disappearing of singlet in Mössbauer spectra in nanocomposites with the largest concentrations of metallic phase.

4. CONCLUSIONS

Electrical properties and hyperfine parameters of Mössbauer spectra of nanocomposites $(Co_{0.45}Fe_{0.45}Zr_{0.10})_X(Al_2O_3)_{1-X}$ with 30 at.%<X<65 at.% show the presence of two critical regions for metallic fraction (X_1 = 33 - 40 at.% and X_2 = 50 - 55 at.%) where 'property-composition' dependences exhibit peculiarities in shape of sudden change of properties. The behavior is attributed to the peculiarities of the distribution of the metallic nanoparticles in the dielectric matrix.

REFERENCES

[1] Yu.E. Kalinin, A.N. Remizov and A.V. Sitnikov // *Bulletin of Voronezh State Technical Univer-*

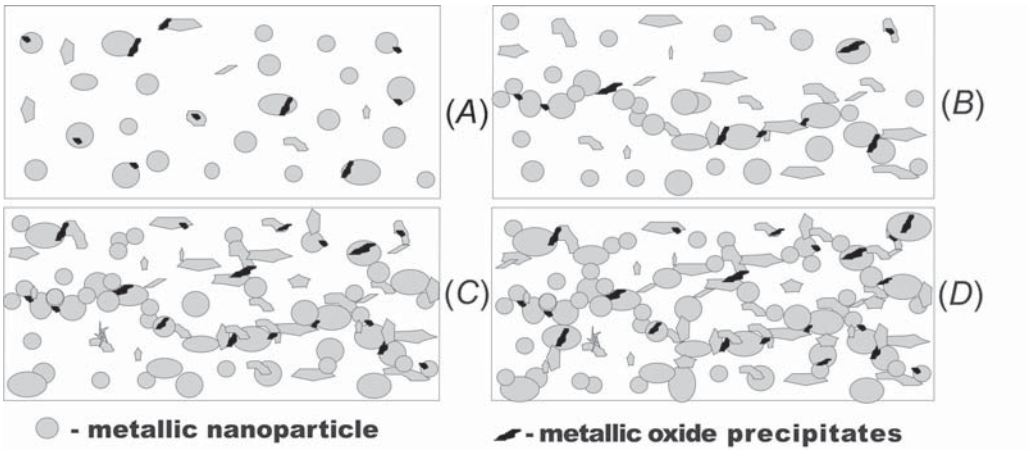

Fig. 8. A schematic sketch of nanocomposite structure for different concentrations of metallic phase: $X < X_1$ (A), $X = X_1$ (B), $X_1 < X < X_2$ (C) and $X > X_2$ (D).

sity: Material Science **N113** (2003) 43, in Russian.
[2] D.G. Rancourt and J.Y. Ping // *Nucl. Instrum. Meth.* **B58** (1991) 85.
[3] A.K. Bandyopadhyay, J. Zarzycki, P. Uric and J. Chappert // *J. Non-Cryst. Solids* **40** (1980) 353.
[4] A. Santos, J.D. Ardisson, A.D.C. Viegas, J.E. Schmidt, A.I.C. Persiano and W.A.A. Macedo // *J. Magn. Magn. Mater.* **226-230** (2001) 1861.
[5] A. Paesano Jr., C.K. Matsuda, J.B.M. da Cunha, M.A.Z. Vasconsellos, B. Hallouche and S.L. Silva // *J. Magn. Magn. Mater.* **264** (2003) 264.
[6] N.F. Mott and E.A. Devis, *Electron processes in noncrystalline materials* (Clarendon Press, Oxford, 1979).
[7] A.L. Efros and B.I Shklovski // *Phys. Stat. Sol. (b)* **76** (1976) 475.
[8] R.M. Hill // *Phil. Mag.* **24** (1971) 1307.
[9] J. Inoe and S. Markava // *Phys. Rev. B* **53** (1996) R11927.